Ciência/Science

OBTAINING TEMPERATURE FIELDS AS A FUNCTION OF EFFICIENCY IN TIG WELDING BY NUMERICAL MODELING

P. B. Guimarães[a,b],

P. M. A. Pedrosa[b],

Y. P. Yadava[b],

A. V. Siqueira Filho[b],

J. M. A. Barbosa[b],

and R. A. S. Ferreira[b]

[a] Instituto Federal de Pernambuco

Departamento de Mecânica

Cidade Universitária

CEP. 50740-540, Recife, Pernambuco, Brasil

pabloguimaraes@recife.ifpe.edu.br

[b] Universidade Federal de Pernambuco

Departamento de Engenharia Mecânica

Cidade Universitária

CEP. 50.740-530, Recife, Pernambuco, Brasil

ras@ufpe.br

ABSTRACT

The temperature field serves as the basis for predicting levels of residual stress in a welded joint. The aspects related to the mathematical modeling of complex welding procedures were pondered with the FEM: variations in the physical and mechanical properties of the materials as a function of the temperature, the transience and the speed of the welding process, the material phase transformations, the different mechanisms of heat exchange with the environment (convection and radiation), all them associated with a high level of nonlinearity. The heat source used in this analytical model for heat supply was the double ellipsoid model proposed by Goldak (2005), in which a 60 mm x 50 mm and 3 mm rectangular ASTM AH36 steel plate was used for the TIG process simulations. It was made a comparison of temperature fields for three different values of process efficiency (60%, 70% and 80%). The results showed many differences in the temperature fields following changes in the levels of residual stresses which will be determined in further studies.

Keywords: Temperature Field, Residual Stress, TIG Welding.

NOMENCLATURE

a_f length of the weld pool before the torch, m
a_r length of the weld pool after the torch, m
b semi-width of the weld pool, m
c depth of fusion zone, m
c_p specific heat at constant pressure, J/kg.ºC
f_f departments of energy before the torch
f_r departments of energy after the torch
h convective heat transfer coefficient, W.m^2/ºC
h_p thickness of the plate, m
K thermal conductivity, W.m/ºC
K_0 modified Bessel function
I electrical current, A
U voltage, V
T_0 initial temperature, ºC
T temperature, ºC
v welding speed, m/s

Greek symbols

α thermal diffusivity, m^2/s
ε emissivity
σ Stefan-Boltzmann's constant, W.m^{-2}.ºC^{-4}

INTRODUCTION

The TIG (Tungsten Inert Gas) welding technique begins with the creation and maintainance of the electric arc between a non-consumable tungsten electrode and a base metal (Modenesi et al., 2006; Gonçalves et al., 2006). This welding process was first developed by the aeronautical industry during the World War II to make easier the weld process of light materials such as aluminum and magnesium. After the improvement, TIG became a process of high quality and relatively high cost used in various applications (Marques et al., 2007). In this study, the temperature fields were numerically developed considering three different levels of electrical current in order to obtain the residual stresses of a welded joint subsequently. This numerical model is based on the coupling of different physical phenomena in thermal, mechanical and metallurgical natures, always present in a welding operation. In the 4th decade of the twentieth century, an analytical method was proposed by Rosenthal (1941) to solve the thermal problem, taking into consideration a concentrated heat source (punctual or linear). For the analytical solutions Rosenthal proposed the following simplifying assumptions (Ramanzini et al., 2006 and Goyal et al., 2009): The heat source (punctual, linear) moving at a constant speed along a plate; the physical properties of the medium (part) are constant; heat loss through the surface (convection) are negligible; welding is long enough to reach the quasi-steady state (constant temperature distribution to the observer placed at the heat source) and the phase transformations are negligible. For the modeling of thin plates, the

temperature distribution is constant for the observer who moves along a linear heat source with constant velocity, as shown in Figure 1.
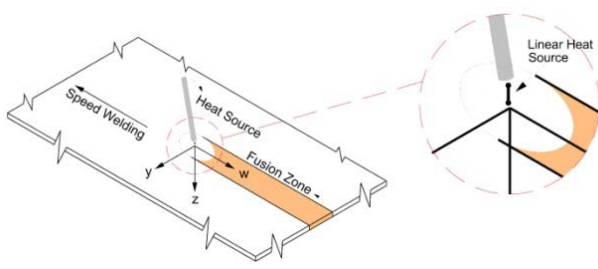

Figure 1. Heat source for linear analysis of two-dimensional heat flow.

Considering that there is no flow in the plate thickness direction and shifting the origin of coordinates of the plate for the linear heat source, the heat conduction takes place in the x and y directions, featuring a bi-directional flow (Binda et al., 2004; Gonçalves et al., 2006).

$$T = T_0 + \frac{P/h_p}{2\pi k} e^{-\frac{v}{2\alpha}x} K_0 \cdot \frac{v}{2\alpha} \cdot \sqrt{x^2 + y^2} \qquad (1)$$

Taking as reference the coordinates, the temperature of a point at a distance r (x, y) has a solution given by Equation (1).

where α is the thermal diffusivity, k is the thermal conductivity, h is the thickness of the plate and v is the welding speed. According Depradeux (2003), these analytical models are well suited only when the size of the fusion is considered a zone very small as compared with the dimensions of the piece. New analytical solutions have been proposed, in which take into account a heat source distributed (Fassani and Trevisan, 2003). For modeling the heat source proposed by Goldak, conduces to an analytical solutions that is currently the most suitable for TIG processes, where is considered a 3D finite Gaussian over a double ellipsoid, as shown in Figure 2.
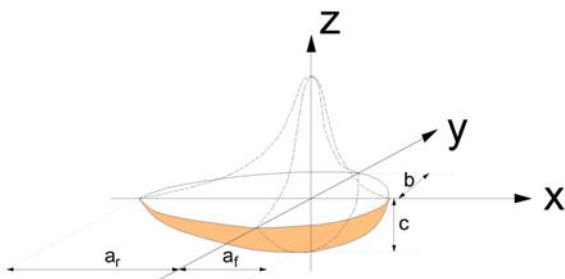

Figure 2. Schematic representation of the double ellipsoid heat source.

$$q_f(x,y,z) = f_f \frac{\eta U I}{a_f bc\pi\sqrt{\pi}} \cdot 6\sqrt{3} \cdot \exp\left(\frac{-3x^2}{a_f^2}\right) \cdot \exp\left(\frac{-3y^2}{b^2}\right) \cdot \exp\left(\frac{-3z^2}{c^2}\right) (2)$$

$$q_r(x,y,z) = f_r \frac{\eta U I}{a_f bc\pi\sqrt{\pi}} \cdot 6\sqrt{3} \cdot \exp\left(\frac{-3x^2}{a_r^2}\right) \cdot \exp\left(\frac{-3y^2}{b^2}\right) \cdot \exp\left(\frac{-3z^2}{c^2}\right) (3)$$

This source is defined analytically by Equation (2) and Equation (3) (Goldak and Chakravarti, 1984; Goldak and Akhlaghi, 2005).

Where q_f and q_r are the volumetric energy distributions before and after the torch [w/m^3]; f_f and f_r are the departments of energy before and after the torch; a_f and a_r are the length of the weld pool before and after the torch [m]; b is the semi-width of the weld pool [m] and c is the depth of fusion zone [m] as shown in Figure 2.

The U and I parameters are linked directly to the welding procedure, while b and c are the geometrical parameters of the source, which may be determined by metallographic examination.

$$f_f + f_r = 2 \qquad (4)$$

$$f_f = \frac{2 \cdot a_f}{a_f + a_r} \qquad (5)$$

$$fr = \frac{2 \cdot a_r}{a_f + a_r} \qquad (6)$$

The other parameters a_f, a_r, f_f and f_r, are obtained by helping of parameters b and c which are related in the bibliography, as shown on Equations (4), (5) and (6) (Gery et al., 2005; Goldak and Akhlaghi, 2005).

EXPERIMENTS

For the simulation of residual stresses, a 60mm x 50mm and 3mm rectangular ASTM AH36 steel plate was used, considering the use of a TIG (tungsten inert gas) in the welding process. Table 1 shows the chemical composition of the alloy.

Table 1. Chemical composition of the sample of ASTM AH36.

C	Cr	Mn	Ni	Si	V
0.130	0.026	1.418	0.012	0.346	0.056
Al	**Cu**	**S**	**P**	**Sn**	**Nb**
0.028	0.015	0.007	0.023	0.002	0.020

Numerical simulations were performed with a software program (Abaqus) based on the finite element method (FEM). The board was divided into elements type DC3D8 sum to a total of 18788 elements. This mesh presented more refinement in the fusion zone and in the heat affected zone (HAZ), because those were the areas where the most important phenomena in the welding process

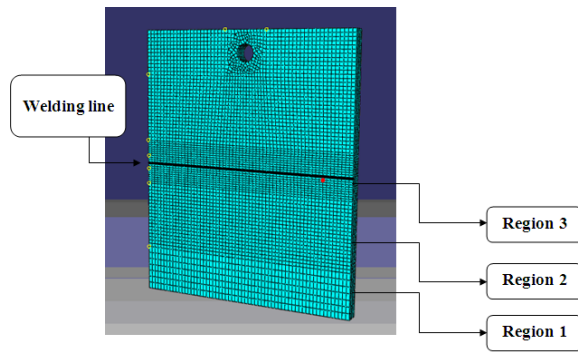occurred. This mesh refinement is shown in Figure 3 and in Table 2.

Figure 3. Mesh and regions used for problem solving thermal and mechanical.

Table 2. Elements that make up the mesh for the FEM calculation.

	Region 1	Region 2	Region 3
Number of Elements	4336	9272	4880

These elements are continuous - 3D of linear formulation and each one of them contains 8 nodes (Figure 4). For all elements, edges along the 0,75mm thick were always used, remaining four elements along the thickness of the plate.
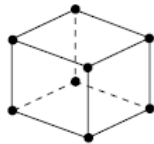

Figure 4. Element DC3D8 - 8 nodes and linear formulation (Hibbit et al., 2007).

$$\frac{\partial}{\partial x}\left(K_T\,\frac{\partial T}{\partial x}\right)+\frac{\partial}{\partial y}\left(K_T\,\frac{\partial T}{\partial y}\right)+\frac{\partial}{\partial z}\left(K_T\,\frac{\partial T}{\partial z}\right)+\dot{q}=\rho c\,\frac{\partial T}{\partial t} \quad (7)$$

The solution of the thermal problem is given by Equation (7).

For the thermal boundary conditions, the exchange of convection and radiation was considered during the welding process. These boundary conditions were imported to the model. Five sides of the plate were welded, except the lower surface, which rested on the table during the welding operation.

$$q_c = h\left(T - T_0\right) \quad (8)$$

$$q_R = \sigma \cdot \varepsilon \cdot \left(T^4 - T_\infty^4\right) \quad (9)$$

Heat exchange by convection and radiation was expressed by Eq. (8) (Newton's law) and Eq. (9) (Stefan Boltzmann's law), respectively.

Where h is the convection coefficient, σ is the Stefan-Boltzmann's constant and ε represents emissivity. Literature values were used to model heat exchange and the assumed convection around the board. The ambient temperature considered was 25° C and emissivity 0.7. The values used for the convection coefficient (h), specific heat (C_p) and thermal conductivity (k) are shown in Figure 5 (Tsirkas et al. 2003) as a function of temperature.
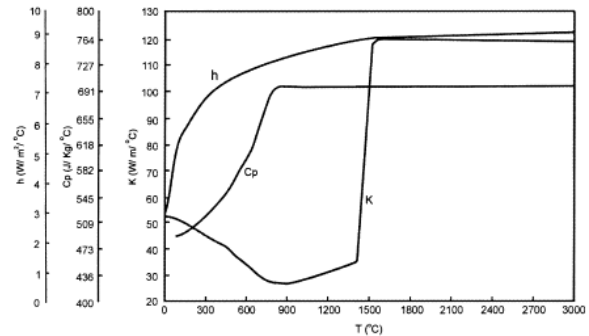

Figure 5. Variation of material properties as a function of temperature (tsirkas et al., 2003).

The source used in this study was the double ellipsoid model proposed by Goldak, shown in Figure 2. The geometric parameters a_f, a_r, b, c and the energy parameters f_f and f_r were obtained with the support of the relationships found in references suggested by Gery et al (2005) and Goldak et al. (2005) (Table 3). During the modeling, a FORTRAN DFLUX subroutine (Hibbit et al. 2007) was developed to displace the heat source. This function determines the torch position versus time, and calculates the heat input in all points of the board. Only one mechanical boundary condition was established because the plate was attached through a 4 mm diameter hole, as shown in Figure 2 (Danis et al. 2008).

Table 3. Geometrical parameters and energy from the heat source (Goldak & Akhlaghi, 2005; Danis, 2008).

Parameter	Value
a_f	0.0025m
a_r	0.0015m
b	0.0025m
c	0.003m
f_f	0.6
f_r	1.4

For the numerical simulations performed, in this study the value of the voltage and electrical current were kept constant and equal to 14 V and 152 A respectively. The variations in efficiency source were applied, as shown in Table 4.

Table 4. Parameters of heat input used in the numerical simulation.

Current (A)	Voltage (V)	Efficiency (%)	Speed (m/s)
152	14	60	0.001
152	14	70	0.001
152	14	80	0.001

RESULTS AND DISCUSSION

The virtual welding lasted 50s. The evolution of temperature field for efficiency source of 60%, 70% and 80% are shown in the Figures 6, 7 and 8 respectively.
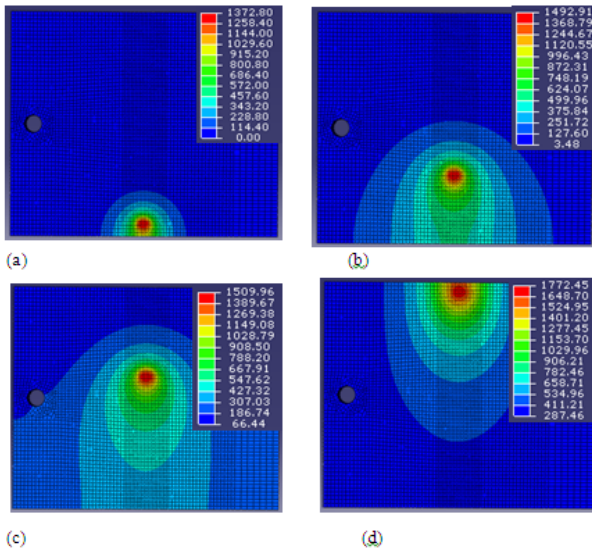

Figure 6. Evolution of the field of temperature [ºC] for efficiency source of 60% as a function of the welding times (a) 5 s, (b) 15 s, (c) 30 s and (d) 50 s.
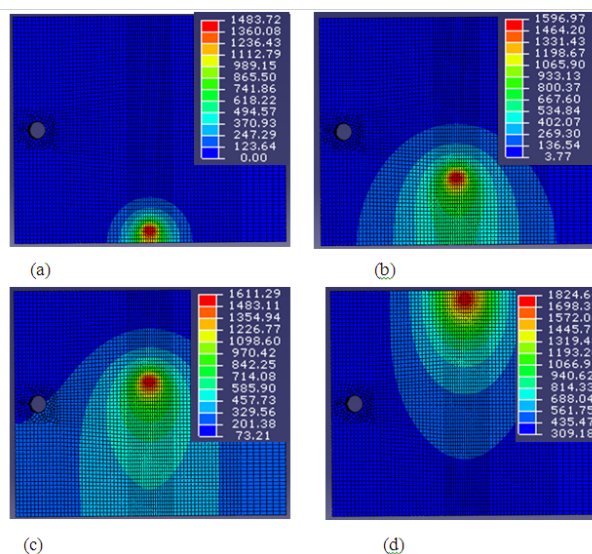

Figure 7. Evolution of the temperature field [ºC] for efficiency source of 70% as a function of the welding times (a) 5 s, (b) 15 s, (c) 30 s and (d) 50 s.
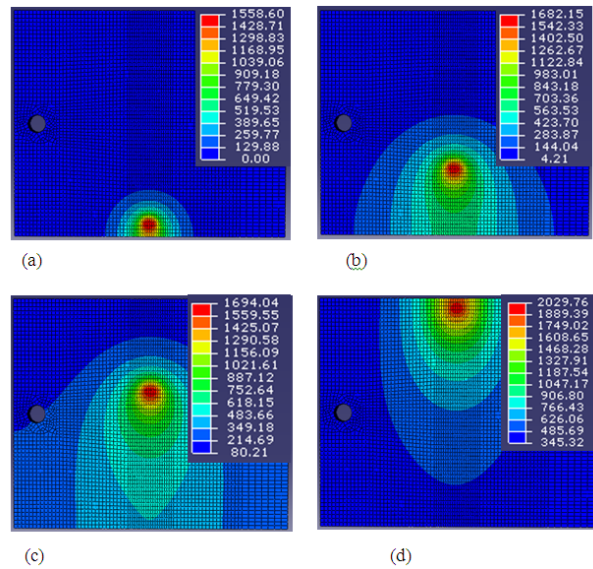

Figure 8. Evolution of the temperature field [ºC] for efficiency source of 80% as a function of the welding times (a) 5 s, (b) 15 s, (c) 30 s and (d) 50 s.

The evolution of the temperature field is influenced by the parameters of the heat source and the heat input welding. The contours of this field are directly influenced by the welding speed and the physical properties of the material. For simulations, a welding speed of 1 mm/s was used. Under these conditions (Figures 6, 7 and 8), the Heat Affected Zone (HAZ) is higher for the current of 162A, due to the increase in heat input. If the speed of welding increases the contours of the isotherms tend to stretch more towards the opposite direction to welding, thus affecting a smaller area (Chon and Chin, 1993), however the welding speed in this work was kept constant. In this model the temperature remains nearly constant over the thickness, according to the problem solution for thin plate proposed by Rosenthal (1941).

The maximum temperature achieved for the welding efficiency of 60% was 1772° C, for the welding efficiency of 70% was 1824º C and for the efficiency of welding of 60% was 2029º C.

In literature, models that do not take into account the phase transformations (γ-α) of material can be easily found, but they present poor accuracy in results concerning the temperature field. In this study, phase transformations were considered but these simulated results are in accordance with experimental results (Guimarães, 2010).

CONCLUSIONS

The determination of the temperature field in welding produced by TIG can be simulated by using the *Abaqus code* in which both thermal and mechanical effects can be considered as well. Considering the phase transformation (γ–α) during

virtual welding, the model presented consistent results under the experiment.

The determination of the temperature field can be used either for the optimization of welding procedures in future works or in reducing the levels of residual stress in different industrial range, such as in the petrochemical and shipbuilding industries.

ACKNOWLEDGEMENTS

REFERENCES

Binda, B., Capello, E. and Previtali, B., 2004, A semi-empirical model of the temperature field in the AISI 304 laser, welding Journal of Materials Processing Technology. Vol. 155, pp. 1235–1241.

Chon, L. T. and Chin, M. T., 1993, Heat Flow in Fusion Welding - Parametric Effects, ASM HANDBOOK. Vol. 6, pp. 46-53.

Danis, P. Y., 2008, Étude de la soudabilité d'um superalliage base nickel fortement charge em éléments durcissants titane et aluminium: l'inconel 738, Doctoral Thesis, L'Université Bordeaux 1, France.

Depradeux, L. and Jullien, J. F., 2003, Experimental and numerical simulation of thermomechanical phenomena during a TIG welding process, *In: International Conference on Thermal Process Modelling and Computer Simulation*. Nancy, France, pp. 697-704.

Fassani, R. N. S. and Trevisan, O. V., 2003, Analytical Modeling of Multipass Welding Process with Distributed Heat Source, Journal of the Braz. Soc. of Mech. Sci. & Eng. Vol. XXV, No. 3, pp. 302-305.

Gery, D., Long, H. and Maropoulos, P., 2005, Effects of welding speed, energy input and heat source distribution on temperature variations in butt joint welding, Journal of Materials Processing Technology. Vol. 167, pp. 393–40.

Goldak, J. A. and Akhlaghi, M., 2005, *Computational Welding Mechanics*, Spring, New York.

Gonçalves, C. V., Vilarinho, L. O., Scotti, A. and Guimarães, G., 2006, Estimation of heat source and thermal efficiency in GTAW process by using inverse techniques, Journal of Materials Processing Technology . Vol. 172, pp. 42-51.

Goyal, V. K., Ghosh, P. K. and Saini, J. S., 2009, Analytical studies on thermal behaviour and geometry of weld pool in pulsed current gas metal arc welding, Journal of materials processing technology. Vol. 209, pp.1318-1336.

Guimarães, P. B., 2010, Estudo do Campo de Temperatura Obtido Numericamente para Posterior Determinação das Tensões Residuais em uma Liga de Aço ASTM AH36, Doctoral Thesis, Universidade Federal de Pernambuco, Brazil. (in Portuguese)

Hibbit, Karlsson & Sorenson Inc., 2007, *Abaqus User Subroutines Reference Manual version 6.7*, USA.

Hibbit, Karlsson & Sorenson Inc., 2007, *Abaqus Getting Started with Abaqus* – Interactive Edition version 6.7, USA.

Marques, P. V., Modenesi, P. J., Bracarense, A.Q., 2007, *Soldagem: Fundamentos e Tecnologia*. Ed. UFMG, Belo Horizonte, Brazil. (in Portuguese)

Modenesi, P. J., Marques, P. V. and Santos, D. B., 2006, *Introdução à Metalurgia da Soldagem*. Universidade Federal de Minas Gerais. DEM, Belo Horizonte, Brazil. (in Portuguese)

Ramanzini, R. and Paucar Casas, W. J., 2006, Distribuição do Campo de Temperaturas num Protótipo Virtual de Junta Soldada Multipasse, in: *17º CBECiMat - Congresso Brasileiro de Engenharia e Ciência dos Materiais*. PR, Brazil. pp. 7791-7800. (in Portuguese)

Rosenthal, D., 1941, Mathematical theory of heat distribution during welding and cutting, Weld. J. Vol. 20, pp. 220–234.

Tsirkas, S. A., Papanikos, P. and Kermanidis, T.H., 2003, Numerical Simulation of the Laser Welding Process in butt-joint specimens, Journal of Materials Processing Technology. Vol. 134, pp. 59-69.